

COVER PAGE

Document downloaded by @DAEL

Sat Nov 21 20:54:19 2026
For personal use

When automatic English translation is provided, only the original document is authentic.
The EAA cannot be held responsible of any translation error

Bibliographical reference

Validation of the Sample Rotation Scheme in the Measurement of Random-Incidence Scattering Coefficients, Tetsuya Sakuma and Hyojin Lee, Acta Acustica **vol. 99** (Number 5), 2013, pp. 737-750

DOI
https://doi.org/10.3813/AAA.918652

ACTA ACUSTICA UNITED WITH ACUSTICA
Vol. 99 (2013) 737 – 750
DOI 10.3813/AAA.918652

Validation of the Sample Rotation Scheme in the Measurement of Random-Incidence Scattering Coefficients

Tetsuya Sakuma, Hyojin Lee
Graduate School of Frontier Sciences, The University of Tokyo 5-1-5 Kashiwanoha, Kashiwa, Chiba 277-8563, Japan. sakuma@k.u-tokyo.ac.jp

Summary
The reverberation room method for measuring random-incidence scattering coefficients, standardized by ISO 17497-1, employs a sample rotation scheme to extract specularly reflected energy, where synchronized averaging of room impulse responses is performed during stepwise or continuous rotation of a test sample. However, the requirements of the stepwise and the continuous approaches are not yet clarified, particularly the latter employing the correlation technique with periodic pseudo-random signals. This paper theoretically elucidates the principles of the two approaches and formulates the error in scattering coefficient measured by each approach. Theoretical analyses demonstrate the minimum number of angular steps and the minimum revolution period that depend on the sample's scattering coefficient and the room's absorption area. Small- and full-scale experiments on the continuous approach verify that the minimum revolution period exists in the use of maximum-length sequence signals, however, the minimum number of signals exists in the use of swept sine signals, corresponding to angular steps in the stepwise approach.

PACS no. 43.20.Fn

1. Introduction

Since surface scattering plays a significant role in determining acoustic quality of rooms, its applications have been seen in a variety of architectural spaces such as concert halls, auditoria, sound studios, reverberation chambers and so on [1, 2]. Up to now, as an index to evaluate reflection characteristics from surfaces, the scattering coefficient, defined as the ratio of non-specularly reflected to total reflected energy [3, 4], has been widely used because of its usefulness for geometrical room acoustics simulation [5, 6]. Most commercial simulation programs, such as ODEON [7], CATT-Acoustic [8] and so on, have incorporated diffuse reflections into geometrical acoustics models by using the scattering coefficient.

The reverberation room method for measuring random-incidence scattering coefficients has been standardized by ISO 17497-1 [9], which is based on the original work by Vorländer and Mommertz [3], and well established by the following works on the effects of sample geometry and mounting, room condition and time variance [10, 11, 12, 13, 14, 15]. As a special feature, this method employs a sample rotation scheme to extract specularly reflected energy, where synchronized averaging of room impulse responses is performed during stepwise or continuous rotation of a test sample. However, this unique scheme could involve some measurement errors, one of which is due to unclear requirements of the number of angular steps in the stepwise approach and of the revolution speed in the continuous approach.

The ISO standard specifies the continuous approach using a multiple of a periodic pseudo-random signal such as the maximum-length sequence (MLS), where the revolution speed is not limited, although, as an example for full-scale measurement, giving a revolution period of 60 seconds for 12 signals with a period of 5 seconds. As shown in Table I, the previous works have used various combinations of test signal and revolution speed for the continuous and the stepwise approaches in small- and full-scale measurements. Most of the measurement conditions were verified numerically and experimentally in case studies.

However, the example condition specified in the ISO standard cannot be found in Table I, and also has not yet been verified theoretically. In this approach, the specularly reflected component is extracted through the two processes, cross-correlation for each signal period and coherent averaging of impulse responses over one revolution period. Of course there must exist a certain upper limit in revolution speed, but it is not unclear, including whether it depends on the number of signals or the signal period.

The ISO standard alternatively specifies that for the stepwise approach the number of coherent averages should be in the range from 60 to 120, and 72 averages is preferred

Received 16 December 2012,
accepted 21 May 2013.

© S. Hirzel Verlag · EAA

Document downloaded by @DAEL, 2026-11-21 20:54:22 - personal use only

Table I. Measurement conditions in the previous papers. T_S: Signal period [s], N: Number of signals, $\Delta\theta$: Angular interval [deg], T_R: Revolution period [s/rev].

Inst.	Ref.	Scale	Method	Signal type	T_S [s]	N	$\Delta\theta$ [deg]	T_R [s/rev]
A	[3]	1/5	Continuous	MLS	0.85	94	3.8	80
	[11]				1.48	54	6.7	80
B	[12]	1/1	Continuous	Log-SS	20	27	13.3	540
	[13]				16	35	10.3	560
C	[13]	1/1	Stepwise	Log-SS	12	36	10	N/A
D	[21]	1/10	Stepwise	MLS	N/A	72	5	N/A
	[22]		Continuous		0.68	88	4.1	60
E	[14]	1/5	Stepwise	Lin-SS	1.34	72	5	N/A
	[15]		Continuous	Log-SS	1.34	79	4.6	105
F	[23]	1/2	Continuous	MLS	5.1	16	22.5	81.6

corresponding to angular intervals of 5 degrees. This limitation is based on the early experimental study [3], and has been followed seemingly without problems [11, 13, 14], but it has also not yet been completely verified. It is obvious that an insufficient number of averages leads to some underestimation of scattering coefficient, thus the minimum number is of significance. On the other hand, it is well known that a great number of averages can cause another significant error in too long measurements due to time variance of air condition.

As is not specified in the ISO standard, another continuous approach using a multiple of a swept sine (SS) signal is relatively popular [12, 13, 15]. In each impulse response measurement, the post-processing for a SS signal is based on the time modulation technique, which is different from the cross-correlation technique for MLS. During one continuous rotation, a specific frequency component of the SS signal is intermittently generated at an equal interval corresponding to the signal period. Consequently, this continous approach is rather regarded as being similar to the stepwise approach, and it is expected that the number of signals can be limited, corresponding to the number of angular steps in the stepwise approach.

Regarding the above issue on the sample rotation scheme, this paper theoretically and experimentally investigates the requirements of the stepwise and the continuous approaches using MLS and SS signals. In Chapter 2, the two approaches are theoretically modeled, and those requirements are discussed. Chapter 3 describes measurement setups and conditions of the two approaches tested in 1/4 and 1/1 scales. Chapter 4 presents results of experiments and theoretical considerations. Chapter 5 summarizes the findings and discusses the validation of the sample rotation scheme from practical aspects.

2. Theoretical considerations on the sample rotation scheme

2.1. Fundamentals

As illustrated in Figure 1, the scattering coefficient is defined as the ratio of non-specularly reflected (scattered) energy to total reflected energy, which is represented by

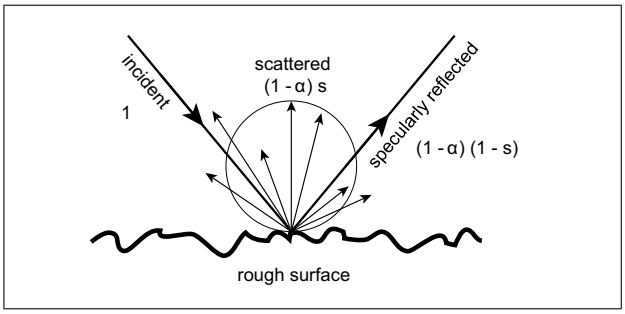


Figure 1. Schematic of the scattering coefficient.

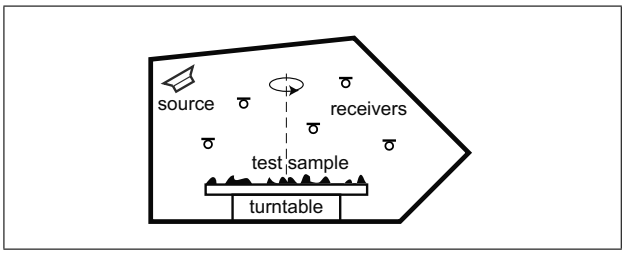


Figure 2. Measurement of random-incidence scattering coefficients in a reverberation room.

$$s = 1 - \frac{E_{\mathrm{spec}}}{E_{\mathrm{total}}} = \frac{\alpha_{\mathrm{spec}} - \alpha_{\mathrm{s}}}{1 - \alpha_{\mathrm{s}}}, \tag{1}$$

where E_{total} and E_{spec} are the total and the specularly reflected energy, α_{s} and α_{spec} are the random-incidence absorption coefficient and the specular absorption coefficient [3]. According to ISO 17497-1, a circular rigid base plate is fixed on a turntable in a reverberation room, and a test sample of an equal area is mounted on the base plate (Figure 2). The above two absorption coefficients are measured for the sample on the basis of ISO 354 [16]; the former is given in the resting state, whereas the latter is given in the rotating state. In practice, the coefficients are calculated by

$$\alpha_{\mathrm{s}} = 24 \ln 10 \frac{V}{S}\left(\frac{1}{c_2 T_2} - \frac{1}{c_1 T_1}\right) - \frac{4V}{S}\left(m_2 - m_1\right), \tag{2}$$

Document downloaded by @DAEL, 2026-11-21 20:54:22 - personal use only

$$\alpha_{\text{spec}} = 24 \ln 10 \frac{V}{S}\left(\frac{1}{c_4 T_4} - \frac{1}{c_3 T_3}\right) - \frac{4V}{S}\left(m_4 - m_3\right), \quad (3)$$

where V is the volume of the reverberation room, S is the area of the test sample, T_i is the reverberation time, c_i is the speed of sound, and m_i is the energy attenuation coefficients of air on the i-th condition of Table III.

In the sample rotation scheme, specularly reflected energy can be extracted by synchronized averaging of the room impulse responses obtained for different sample orientations, assuming statistical independence between scattered components. This scheme is realized during one revolution by means of the stepwise or the continuous approach. As a consequence, the initial energy decay of the averaged impulse response nearly corresponds to the decay of the specularly reflected energy, thus $T_4 \leq T_2$ with the sample, whereas $T_3 \approx T_1$ without the sample. However, a careful evaluation is necessary for T_4 within a level range where the initial decay is linear. The ISO standard specifies that T_4 should be evaluated in the range between -5 dB and -20 dB by using the backward integration method with the integration limit of -30 dB. This specification implies that some measurement conditions to ensure the linearity of the initial decay down to -20 dB are required for the stepwise and the continuous approaches, respectively.

Considering an error involved in the evaluation of T_4, equations (1) and (3) give the related error for the scattering coefficient, as

$$\Delta s = \frac{\Delta \alpha_{\text{spec}}}{1 - \alpha_{\text{s}}} \approx -\frac{\Delta T_4}{T_4} \frac{\alpha_{\text{spec}} + A_1/S}{1 - \alpha_{\text{s}}}, \quad (4)$$

where A_1 is the equivalent absorption area of the room including air absorption. The ISO standard specifies the upper limit for the sample's absorption coefficient, $\alpha_{\text{s}} \leq 0.5$, thus the absolute error can be roughly within the range

$$\frac{A_1}{S}\frac{|\Delta T_4|}{T_4} \leq |\Delta s| \leq \left(1 + \frac{A_1}{S}\right)\frac{|\Delta T_4|}{T_4}. \quad (5)$$

As an example, if a relative error of 5% in T_4 is involved on the room condition that $A_1/S = 1$, the absolute error in scattering coefficient can theoretically reach 0.2 at the greatest for a sample with $\alpha_{\text{s}} = 0.5$ and $s = 1$.

2.2. Stepwise approach

In the stepwise approach, regardless of signal type, one measurement is performed when a test sample is fixed at each angular step, which gives an impulse response for each combination of source and receiver positions. Assuming that the impulse response of the specular and diffuse components [3], the total and the specular energy respponses are modeled on different exponential decays, affected by α_{s} and α_{spec} of a diffuse surface, respectively. Considering the independence between the two components, and eliminating negligible oscillation terms with

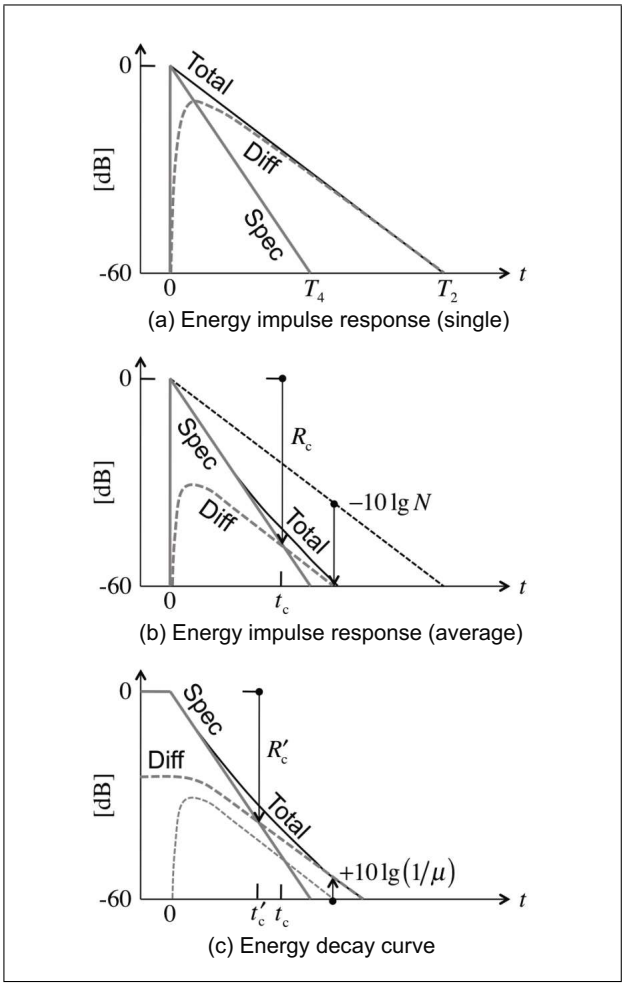


Figure 3. Processing of room impulse responses in the stepwise approach.

time averaging, the energy impulse response for the i-th step is roughly represented by

$$I_{\text{total}}(t) = \left|h_i(t)\right|^2 \approx \left|h_i^{\text{spec}}(t)\right|^2 + \left|h_i^{\text{diff}}(t)\right|^2 = I_{\text{spec}}(t) + I_{\text{diff}}(t), \quad (6)$$

where the total energy $I_{\text{total}}(t) = I_0 \mathrm{e}^{-6\ln(10)t/T_2}$, the specular energy $I_{\text{spec}}(t) = I_0 \mathrm{e}^{-6\ln(10)t/T_4}$, thus the diffuse energy $I_{\text{diff}}(t) = I_0(\mathrm{e}^{-6\ln(10)t/T_2} - \mathrm{e}^{-6\ln(10)t/T_4})$, independently of the sample orientation (Figure 3a).

Further assuming that the specular and the diffuse components respectively correspond to the coherent and the incoherent over the whole measurements, synchronized addition of the impulse responses increases the diffuse and the specular energy proportionally to the number of steps and its square, respectively. Accordingly, the energy decay after averaging of N impulse responses is approximately expressed by

$$\left|\frac{1}{N}\sum_{i=1}^{N} h_i(t)\right|^2 \approx \frac{1}{N}\left(\left|\sum_{i=1}^{N} h_i^{\text{spec}}(t)\right|^2 + \left|\sum_{i=1}^{N} h_i^{\text{diff}}(t)\right|^2\right) \approx I_{\text{spec}}(t) + \frac{1}{N} I_{\text{diff}}(t), \quad (7)$$

Document downloaded by @DAEL, 2026-11-21 20:54:22 - personal use only

where

$$\left|\sum_{i=1}^{N} h_i^{\mathrm{spec}}(t)\right|^2 \approx N^2 I_{\mathrm{spec}}(t), \quad \left|\sum_{i=1}^{N} h_i^{\mathrm{diff}}(t)\right|^2 \approx N I_{\mathrm{diff}}(t).$$

Comparing the two components, $I_{\mathrm{spec}} = I_{\mathrm{diff}}/N$ at the critical time (Figure 3b),

$$t_{\mathrm{c}} = \frac{10\log_{10}(N+1)}{60(1/T_4 - 1/T_2)} = \frac{\log_{10}(N+1)}{6(1-\mu)} T_4, \tag{8}$$

thus the critical decay level of the specular component is represented by

$$R_{\mathrm{c}} = -\frac{10\log_{10}(N+1)}{1-\mu}, \tag{9}$$

where the reverberation ratio $\mu = T_4/T_2 = (\alpha_{\mathrm{s}} + A_1/S)/(\alpha_{\mathrm{spec}} + A_1/S)$, bounded by $1/(1+S/A_1) \le \mu \le 1$.

Furthermore, the energy decay curves for the two components are obtained by the backward integration method, as (Figure 3c)

$$E_{\mathrm{spec}}(t) = \int_t^\infty I_{\mathrm{spec}}(\tau)\,\mathrm{d}\tau = I_0 \frac{T_4 \mathrm{e}^{-6\ln(10)t/T_4}}{6\ln 10}, \tag{10}$$

$$E_{\mathrm{diff}}(t) = \int_t^\infty \frac{1}{N} I_{\mathrm{diff}}(\tau)\,\mathrm{d}\tau = I_0 \frac{T_2 \mathrm{e}^{-6\ln(10)t/T_2} - T_4 \mathrm{e}^{-6\ln(10)t/T_4}}{6\ln(10)N}. \tag{11}$$

Here, on the condition that $E_{\mathrm{spec}} = E_{\mathrm{diff}}$, the critical time and the critical decay level are changed by

$$t_{\mathrm{c}}' = t_{\mathrm{c}} + \frac{\log_{10}\mu}{6(1-\mu)} T_4, \tag{12}$$

$$R_{\mathrm{c}}' = R_{\mathrm{c}} - \frac{\log_{10}\mu}{1-\mu}. \tag{13}$$

Regarding the total energy, equations (10) and (11) lead to

$$E_{\mathrm{total}}(t) = \frac{I_0}{6\ln 10}\left[\left(1 - \frac{1}{N}\right) T_4 \mathrm{e}^{-6\ln(10)t/T_4} + \frac{1}{N} T_2 \mathrm{e}^{-6\ln(10)t/T_2}\right], \tag{14}$$

thus its decay level is represented by

$$R_{\mathrm{total}}(t) = 10\log_{10}\frac{E_{\mathrm{total}}(t)}{E_{\mathrm{total}}(0)} = R_{\mathrm{spec}}(t) + 10\log_{10}\frac{(N-1)\mu + 10^{(\mu-1)R_{\mathrm{spec}}(t)/10}}{(N-1)\mu + 1}, \tag{15}$$

where the decay level of the specular component $R_{\mathrm{spec}}(t) = -60t/T_4$.

In actual measurements, R_{total} can be observed, although R_{spec} is desired to be determined, thus the last term in equation (15) corresponds to the error in the decay evaluation. Supposing that T_4 is estimated in the range from 0 dB to R dB, the error at the bottom level is rewritten by

$$\Delta R = 10\log_{10}\frac{(N-1)\mu + 10^{(\mu-1)(R-\Delta R)/10}}{(N-1)\mu + 1} > 0, \tag{16}$$

Table II. Measurement conditions for the four reverberation times.

Reverberation time	Test sample	Turntable
T_1	not present	not rotating
T_2	present	not rotating
T_3	not present	rotating
T_4	present	rotating

which leads to an error in the reverberant time, $T_4 \approx -(\Delta R/R)T_4$. Recalling equation (4), the resulting error in the scattering coefficient is approximately represented by

$$\Delta s \approx -\frac{1}{\nu}\frac{\Delta T_4}{T_4} \approx \frac{1}{\nu}\frac{\Delta R}{R}, \tag{17}$$

with $\nu = (1-\alpha_{\mathrm{s}})/(\alpha_{\mathrm{spec}} + A_1/S)$ bounded by $0 \le \nu \le S/A_1$, therefore an underestimation always occurs ($\Delta s < 0$). The number of angular steps for the error level ΔR is derived from equation (16) as

$$N = \frac{10^{(\mu-1)(R-\Delta R)/10} - 10^{\Delta R/10}}{\mu(10^{\Delta R/10} - 1)} + 1, \tag{18}$$

consequently, the minimum number for a tolerable error of Δs can be determined by

$$N = \frac{10^{[\mu(1-\nu\Delta s)-1]R/10} - 1}{\mu(1 - 10^{-\nu\Delta s R/10})} + 1. \tag{19}$$

On the condition that $R = -20$ dB in accordance with the ISO standard, the minimum numbers of steps that ensures $|\Delta s| \le 0.05$ for samples with different values of α_{s} and s, are theoretically estimated on different room conditions of A_1/S. As the results shown in Table III, more steps are required as s is greater, while the required number is reduced by increasing α_{s} or A_1/S, that is, unexpectedly by more absorption. The reason can be explained by two effects of increasing the reverberation ratio μ to 1: lowering the critical decay level in the energy impulse response, and suppressing the additional level caused by the backward integration. Figure 4 shows the dependence of the minimum number of steps on s and A_1/S, for the critical sample with $\alpha_{\mathrm{s}} = 0$. It is seen that, at a certain number of steps, the maximum scattering coefficient goes up with increasing A_1. This tendency is quite favorable for actual measurement, since s generally increases at higher frequencies, but A_1 also increases due to air absorption.

The ISO standard prescribes a range of $60 \le N \le 120$, without any minimum equivalent absorption area. However, as shown in Figure 5, the lower limit possibly yields a significant underestimation for a high scattering coefficient in a reverberation room satisfying the rule-of-thumb, $A_1/S \le 1$.

2.3. Continuous approach with pseudo-random signals

In the continuous approach, a multiple of measurements is performed with periodically recurring signals while a test

Document downloaded by @DAEL, 2026-11-21 20:54:22 - personal use only

Table III. Minimum numbers of steps required for $|\Delta s| \leq 0.05$, with changing s and α_s for a test sample, and A_1/S for a reverberation room.

A_1/S	$s = 0.2$	$\alpha_s = 0$	0.2	0.5	$s = 0.5$	$\alpha_s = 0$	0.2	0.5	$s = 1$	$\alpha_s = 0$	0.2	0.5
0.5		11	7	5		78	40	20		411	187	70
1.0		7	6	5		35	24	16		156	95	49
2.0		5	5	4		20	17	13		70	53	36

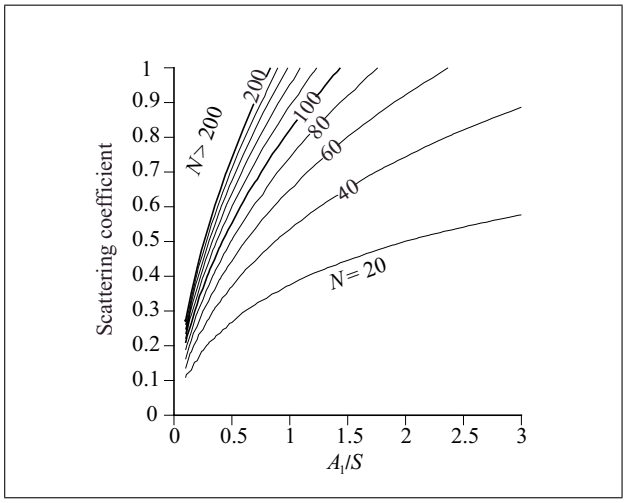


Figure 4. Contours of the minimum number of steps, that ensures $|\Delta s| \leq 0.05$ for the critical sample ($\alpha_s = 0$).

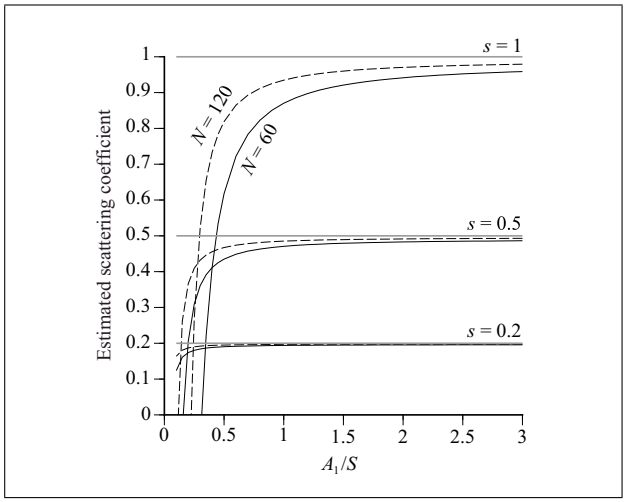


Figure 5. Estimated scattering coefficients for three true values of 0.2, 0.5 and 1, with two typical numbers of steps of 60 and 120.

sample is rotating for one round. If the cross-correlation technique is employed with a pseudo-random signal such as the MLS, one measurement gives an energy impulse response as illustrated in Figure 6a. Here, it is assumed that in each measurement the specular component is localized as the coherent (time-invariant), whereas the diffuse component is spread over the signal period as the incoherent (time-variant), which is apparently transformed into a stationary random noise due to the intra-periodic time-variance effect [17, 18]. Therefore, the energy impulse response for the i-th measurement is represented by

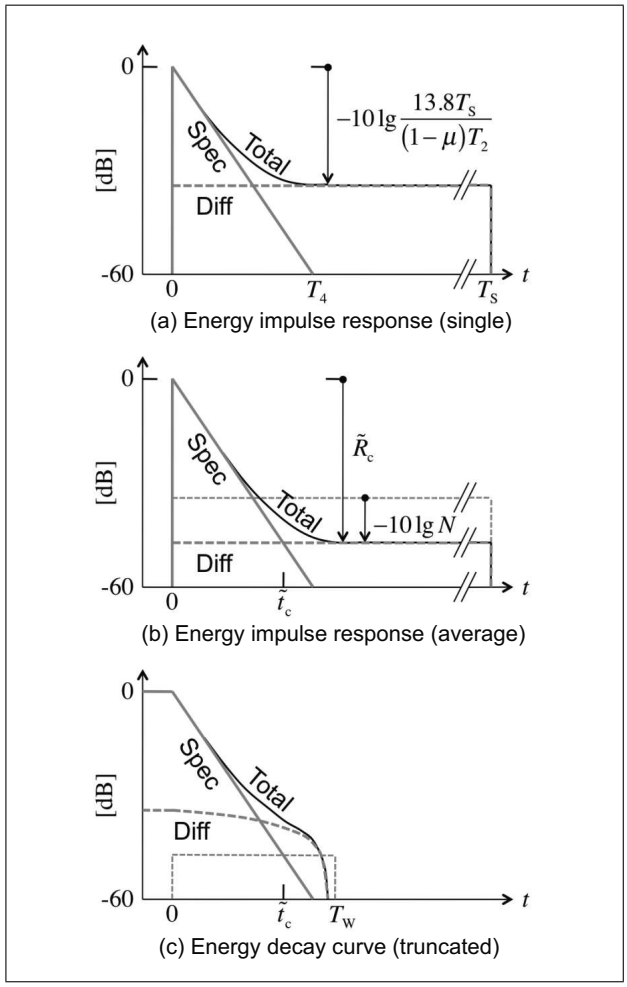


Figure 6. Processing of room impulse responses by the continuous approach with MLS signals.

$$\left|\tilde{h}_i(t)\right|^2 \approx \left|h_i^{\text{spec}}(t)\right|^2 + \left|n_i^{\text{diff}}(t)\right|^2 = I_{\text{spec}}(t) + \overline{I}_{\text{diff}}, \tag{20}$$

where the diffuse energy spread over the signal period T_S, relatively longer than T_2, is approximately expressed by

$$\overline{I}_{\text{diff}} = \frac{1}{T_S}\int_0^{T_S} I_{\text{diff}}(t)\,\mathrm{d}t \approx \frac{1}{T_S}\int_0^{\infty} I_{\text{diff}}(t)\,\mathrm{d}t = I_0\frac{1-\mu}{6\ln 10}\frac{T_2}{T_S}. \tag{21}$$

Again, synchronized addition of the impulse responses increases the specular and the diffuse energy proportion-

Document downloaded by @DAEL, 2026-11-21 20:54:22 - personal use only

ally to N^2 and N, respectively, where N corresponds to the number of signal periods (Figure 6b). Accordingly,

$$\left|\frac{1}{N}\sum_{i=1}^{N} h_i(t)\right|^2 \approx \frac{1}{N^2}\left(\left|\sum_{i=1}^{N}\tilde{h}_i^{\mathrm{spec}}(t)\right|^2 + \left|\sum_{i=1}^{N} n_i^{\mathrm{diff}}(t)\right|^2\right) \approx I_{\mathrm{spec}}(t) + \frac{1}{N}\overline{I}_{\mathrm{diff}}, \tag{22}$$

and the latter component can be expressed by

$$\frac{1}{N}\overline{I}_{\mathrm{diff}} \approx I_0 \frac{1-\mu}{6\ln 10}\frac{T_2}{T_{\mathrm{R}}} = I_0\tilde{r}_{\mathrm{c}}, \tag{23}$$

with the revolution period $T_{\mathrm{R}} = NT_{\mathrm{S}}$. It means that the level of noise floor transformed from diffuse energy depends on the revolution time, but not on the signal period and the number of signals. On the condition that $I_{\mathrm{spec}}(t) = \overline{I}_{\mathrm{diff}}/N$, the critical time is given by $\tilde{t}_{\mathrm{c}} = (-\tilde{R}_{\mathrm{c}}/60)T_4$, where the critical decay level of the specular component is equal to the noise floor level, $R = 10\log_{10}\tilde{r}_{\mathrm{c}}$.

Before the backward integration, the averaged impulse response needs to be truncated at a certain length to reduce the spread diffuse energy. With a truncation time of T_{W}, the energy decay curves for the two components are obtained as (Figure 6c)

$$\tilde{E}_{\mathrm{spec}}(t) = \int_t^{T_{\mathrm{W}}} I_{\mathrm{spec}}(\tau)\,\mathrm{d}\tau = I_0\frac{T_4}{6\ln 10}\left[\mathrm{e}^{-6\ln(10)t/T_4} - \mathrm{e}^{-6\ln(10)T_{\mathrm{W}}/T_4}\right], \tag{24}$$

$$\tilde{E}_{\mathrm{diff}}(t) = \int_t^{T_{\mathrm{W}}} \frac{1}{N}\overline{I}_{\mathrm{diff}}\,\mathrm{d}\tau = I_0\tilde{r}_{\mathrm{c}}(T_{\mathrm{W}} - 1). \tag{25}$$

In the total energy $\tilde{E}_{\mathrm{total}} = \tilde{E}_{\mathrm{spec}} + \tilde{E}_{\mathrm{diff}}$, its decay level is given by

$$\tilde{R}_{\mathrm{total}}(t) = 10\log_{10}\frac{\tilde{E}_{\mathrm{total}}(t)}{\tilde{E}_{\mathrm{total}}(0)} = R_{\mathrm{spec}}(t) + 10\log_{10}\frac{1 - \left[10^{-6\beta} - \frac{\ln 10}{10}\left(60\beta + R_{\mathrm{spec}}(t)\right)\tilde{r}_{\mathrm{c}}\right]10^{-R_{\mathrm{spec}}(t)/10}}{1 - 10^{-6\beta} + 6\ln(10)\beta\tilde{r}_{\mathrm{c}}}, \tag{26}$$

with $\beta = T_{\mathrm{W}}/T_4$. Accordingly, in the decay evaluation, the error level at the bottom level R is given by

$$\Delta\tilde{R} = 10\log_{10}\frac{1 - \left[10^{-6\beta} - \frac{\ln 10}{10}\left(60\beta + R - \Delta\tilde{R}\right)\tilde{r}_{\mathrm{c}}\right]10^{(\Delta\tilde{R}-R)/10}}{1 - 10^{-6\beta} + 6\ln(10)\beta\tilde{r}_{\mathrm{c}}}. \tag{27}$$

Recalling equation (17) for the error of the scattering coefficient, equation (27) is transformed into

$$\tilde{R}_{\mathrm{c}} = 10\log_{10}\left[\frac{10}{\ln 10}\cdot\frac{\left(1 - 10^{-\nu\Delta s R/10}\right)10^{R/10} + 10^{-6\beta}\left(1 - 10^{R/10}\right)}{\left(1 - \nu\Delta s\right)R + 60\beta\left(1 - 10^{R/10}\right)}\right], \tag{28}$$

thus, $\tilde{R}_{\mathrm{c}}$ for a tolerable error of Δs can be determined with a fixed truncation time. Alternatively, supposing that the averaged impulse response is optimally truncated at the critical time ($T_{\mathrm{W}} = \tilde{t}_{\mathrm{c}}$), an implicit formula is given by

$$\tilde{R}_{\mathrm{c}} = 10\log_{10}\left[\frac{10}{\ln 10}\cdot\frac{\left(1 - 10^{-\nu\Delta s R/10}\right)10^{R/10} + 10^{\tilde{R}_{\mathrm{c}}/10}\left(1 - 10^{R/10}\right)}{\left(1 - \nu\Delta s\right)R - \tilde{R}_{\mathrm{c}}\left(1 - 10^{R/10}\right)}\right]. \tag{29}$$

The above equation can be numerically solved, but does not always have a solution of $\tilde{R}_{\mathrm{c}}$. On the condition that $R = -20\,\mathrm{dB}$ and $\tilde{R}_{\mathrm{c}} \le -30\,\mathrm{dB}$, it is numerically verified that an underestimation of Δs occurs if a solution of $\tilde{R}_{\mathrm{c}}$ is given; otherwise the resulting error is within Δs.

Finally, according to equation (23), the minimum revolution period is determined from a tolerable level of $\tilde{R}_{\mathrm{c}}$ by

$$T_{\mathrm{R}} = \frac{1-\mu}{6\ln 10}10^{-\tilde{R}_{\mathrm{c}}/10}T_2. \tag{30}$$

Substituting equation (28) into the above gives the expression

$$T_{\mathrm{R}} = \frac{1-\mu}{\alpha_{\mathrm{s}} + A_1/S}\cdot\frac{\left(1 - \nu\Delta s\right)R/60 + \beta\left(1 - 10^{R/10}\right)}{\left(1 - 10^{-\nu\Delta s R/10}\right)10^{R/10} + 10^{-6\beta}\left(1 - 10^{R/10}\right)}T_0, \tag{31}$$

with the reference reverberation time of the room $T_0 = 24\ln 10(V/c_1 S)$. It is noted that the minimum revolution period is almost proportional to V, thus a larger room requires a longer revolution period.

Again supposing that $|\Delta s| \le 0.05$, the minimum ratios of revolution period to the reference reverberation time are theoretically estimated for different samples and room conditions. Tables IV and V show the results with a typical truncation time $T_{\mathrm{W}} = T_1/2$ that beforehand guarantees more than 30 dB decay for the specular component, and with the optimal truncation time $T_{\mathrm{W}} = \tilde{t}_{\mathrm{c}}$, respectively. With the typical truncation, a longer revolution period is required as s is greater, while it is reduced by increasing α_{s} or A_1/S, similarly to the stepwise approach. With the optimal truncation, the minimum revolution period is remarkably shortened, especially for a less absorptive sample.

Figure 7 shows the dependence of the minimum revolution period ratio on s and A_1/S for the critical sample with $\alpha_{\mathrm{s}} = 0$, employing the typical truncation time $T_{\mathrm{W}} = T_1/2$ and the double time $T_{\mathrm{W}} = T_1$. It is seen that the minimum ratio generally increases more than twice with doubling the truncation time, which implies that the continuous approach with MLS signals is relatively sensitive to truncation of impulse responses. Compared with the minimum number of steps in the stepwise approach (Figure 4), the ISO range of $60 \le N \le 120$ roughly corresponds to $100 < T_{\mathrm{R}}/T_0 < 300$ for $0.5 < A_1/S < 2$ with $T_{\mathrm{W}} = T_1/2$.

Document downloaded by @DAEL, 2026-11-21 20:54:22 - personal use only

Table IV. Minimum ratios of revolution period to the reference reverberation time with a typical truncation time $T_W = T_1/2$, required for $|\Delta s| \leq 0.05$ with changing s and α_s for a test sample, and A_1/S for a reverberation room.

A_1/S	$s = 0.2$	$\alpha_s = 0$	0.2	0.5	$s = 0.5$	$\alpha_s = 0$	0.2	0.5	$s = 1$	$\alpha_s = 0$	0.2	0.5
0.5		67	69	68		311	250	204		1069	753	517
1.0		21	24	27		91	85	78		298	246	194
2.0		6	7	8		26	26	26		87	78	66

Table V. Minimum ratios of revolution period to the reference reverberation time with the optimal truncation time $T_W = \tilde{t}_c$, required for $|\Delta s| \leq 0.05$ ($\tilde{R}_c \leq -30$ dB), with changing s and α_s for a test sample, and A_1/S for a reverberation room. The ratios in parentheses are required for a supplementary condition: $\tilde{R}_c = -30$ dB.

A_1/S	$s = 0.2$	$\alpha_s = 0$	0.2	0.5	$s = 0.5$	$\alpha_s = 0$	0.2	0.5	$s = 1$	$\alpha_s = 0$	0.2	0.5
0.5		(41)	(19)	11		(72)	(38)	32		(97)	(55)	75
1.0		(12)	(7)	10		(24)	18	27		44	53	59
2.0		5	7	8		16	18	21		37	39	43

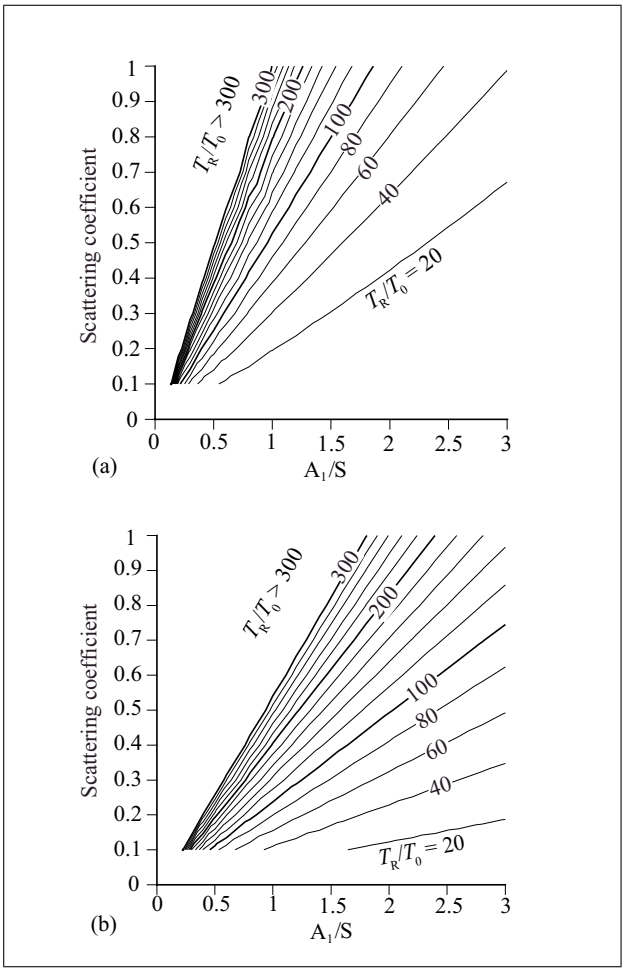


Figure 7. Contours of the minimum revolution period ratio, that ensures $|\Delta s| \leq 0.05$ for the critical sample ($\alpha_s = 0$): (a) with the typical truncation time $T_W = T_1/2$, and (b) with the double time $T_W = T_1$.

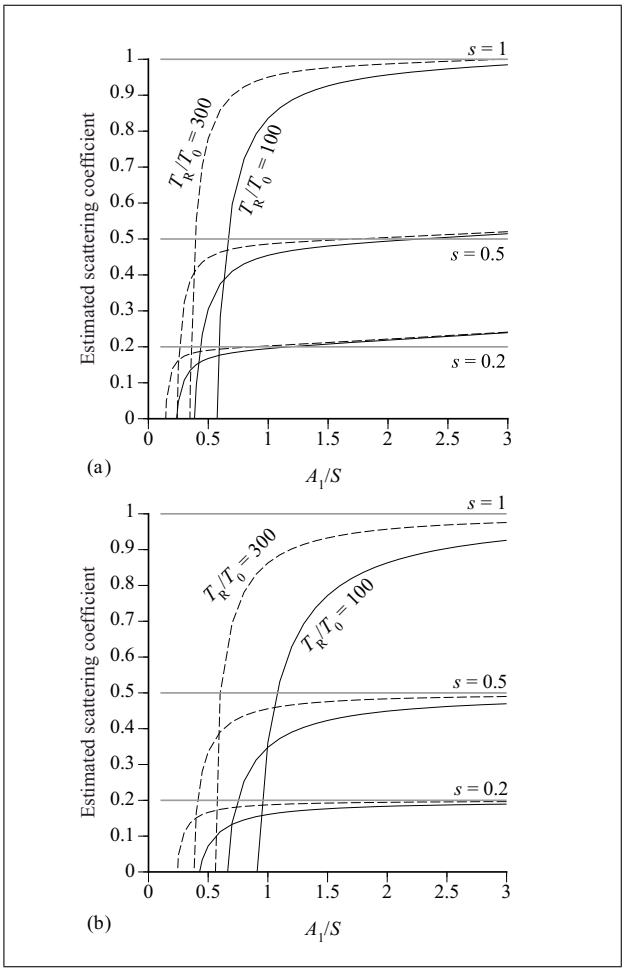


Figure 8. Estimated scattering coefficients for three true values of 0.2, 0.5 and 1, , at two typical revolution period ratios of 100 and 300: (a) with $T_W = T_1/2$, and (b) with $T_W = T_1$.

Figure 8 shows the scattering coefficients estimated with the two revolution period ratios of 100 and 300. As a peculiar feature, it is seen that an overestimation can occur for low scattering coefficients with $T_W = T_1/2$. This is originated from an underestimation of T_4 due to short truncation, which can also occur if employing the same truncation in the stepwise approach.

Document downloaded by @DAEL, 2026-11-21 20:54:22 - personal use only

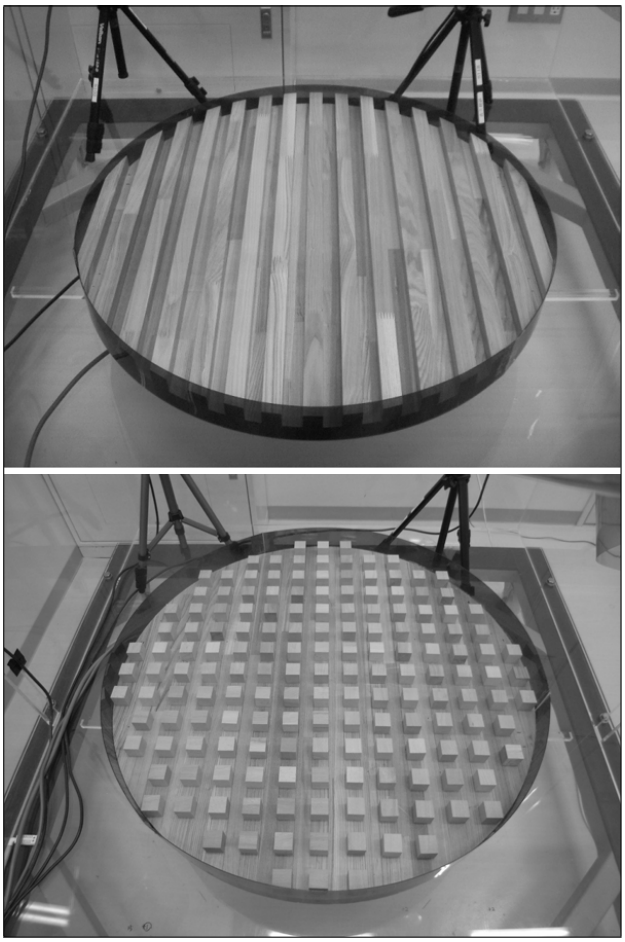


Figure 9. Two types of test samples in 1/4 scale. Top: 1D periodic structure with ribs, and bottom: 2D periodic structure with blocks.

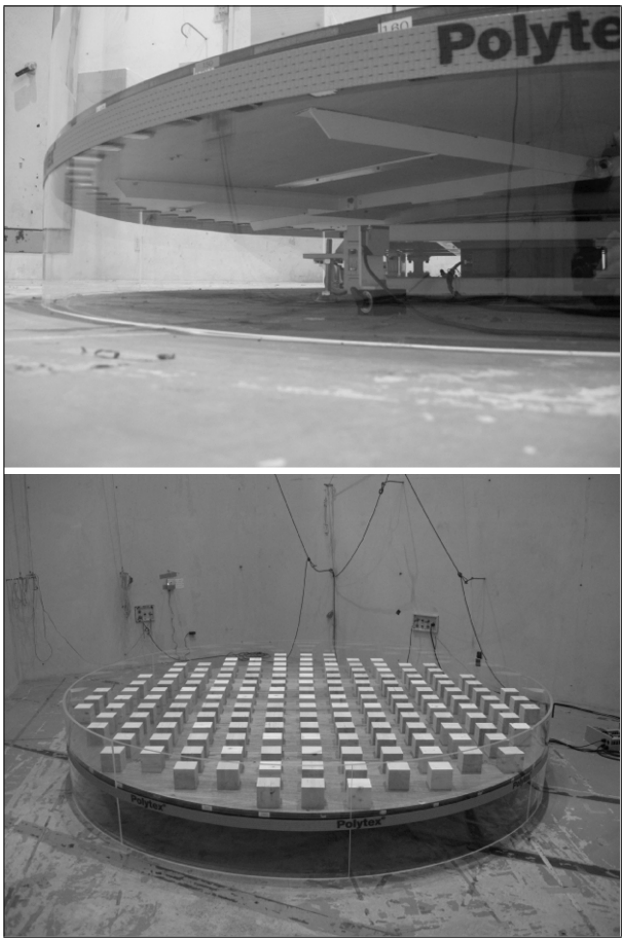


Figure 11. The base plate and the test sample in 1/1 scale. Top: Base plate with the border, and bottom 2D periodic structure with blocks.

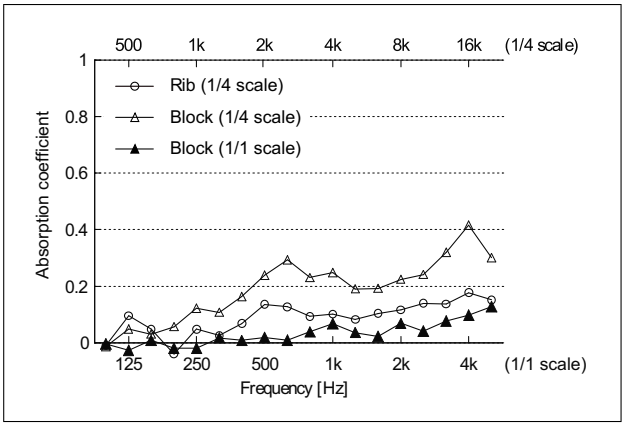


Figure 10. Measured random-incidence absorption coefficients of the test samples in 1/4 and 1/1 scales.

3. Measurement setups in small and full scales

3.1. Test arrangements

Small-scale measurements are performed in a 1/4-scale rectangular reverberation room with a volume of 1.62 m^3 and a surface area of 8.46 m^2, which is made of 10 mm acrylic boards with hanging 10 diffuser panels (1 mm thick plastic). A wooden base plate with a diameter of 750 mm and a thickness of 30 mm is placed on the turntable (Nittobo Acoust. Eng. TT-1000). Additionally, it is surrounded with a plastic border with a thickness of 1 mm and a height of 50 mm to suppress undesirable scattering from the periphery of a test sample [15]. The height of the border is slightly greater than 1/16 of the diameter of the base plate, that is the maximum structural depth for test samples by ISO 17497-1. Two types of samples with one- and two-dimensional periodic structures are tested as shown in Figure 9. The 1D periodic structure is composed of 15 square ribs, and the 2D periodic structure is composed of 161 cubic blocks, both of which are made of wood, with a height of 25 mm and a period of 50 mm. Figure 10 shows the measured random-incidence absorption coefficients of the two samples.

Full-scale measurements are performed in a non-rectangular reverberation room with a volume of 270 m^3, a surface area of 255 m^2, and no diffuser panels. This room is relatively large, and about 2.6 times the volume of the above small-scale room, 104 m^3 with scale conversion. A wooden base plate with a diameter of 3 m and a thickness of 45 mm is placed on a self-made turntable, and sur-

Document downloaded by @DAEL, 2026-11-21 20:54:22 - personal use only

Table VI. Conditions of the impulse response measurements in 1/4 scale. T_S: Signal period [s], N: Number of signals, $\Delta\theta$: Angular interval [deg].

T_S	Revolution period [s/rev]						
0.68	-	-	10.2	20.5	41.0	81.9	164
1.37	-	10.9	20.5	41.0	81.9	164	328
2.73	10.9	21.8	41.0	81.9	164	328	-
5.46	21.8	43.7	81.9	164	328	-	-
10.9	43.7	87.4	164	328	-	-	-
21.8	87.4	175	328	-	-	-	-
$\Delta\theta$	90	45	24	12	6	3	1.5
N	4	8	15	30	60	120	240

Table VII. Conditions of the impulse response measurements in 1/1 scale. T_S: Signal period [s], N: Number of signals, $\Delta\theta$: Angular interval [deg].

T_S	Revolution period [s/rev]				
2.73	-	81.9	164	328	655
5.46	81.9	164	328	655	1311
10.9	164	328	655	1311	-
$\Delta\theta$	24	12	6	3	1.5
N	15	30	60	120	240

rounded with an acrylic border (210 mm height above the plate, 10 mm thickness). As shown in Figure 11, the border is fixed on the floor to suppress not only edge scattering above the plate but also undesirable effects of mechanical noise and moving beams below the plate. One type of sample is tested, which has a similar profile to the 2D periodic structure in the 1/4-scale study, composed of 161 blocks (100 mm height, 200 mm period). However, its absorption coefficients are generally lower than those in 1/4 scale as shown in Figure 10.

3.2. Conditions of impulse response measurements

The continuous approach is examined on a variety of conditions of impulse response measurements with MLS and SS signals of an equal power level. Tables VI and VII show the measurement conditions in 1/4 and 1/1 scales, respectively, where changing the signal period and the revolution period. Accordingly, the number of signals per revolution and the angular interval per signal are inversely changed. For the source and receiving equipment, three and four microphones are placed with two loudspeakers in 1/4 and 1/1 scales, that is, impulse responses for six and eight paths are measured, respectively. The measurements are performed $15/N$ minutes later after closing the door in $1/N$ scale.

Figure 12 shows the measured reverberation times T_1 and the equivalent absorption areas A_1 of the two reverberation rooms. It is seen that the measured absorption areas including air absorption are greater than the sample's area S at high frequencies in both scales. In ISO 17497-1, it is specified that the empty room should satisfy that $A_1 \leq 0.3V^{2/3}$. The 1/1-scale room almost satisfies the

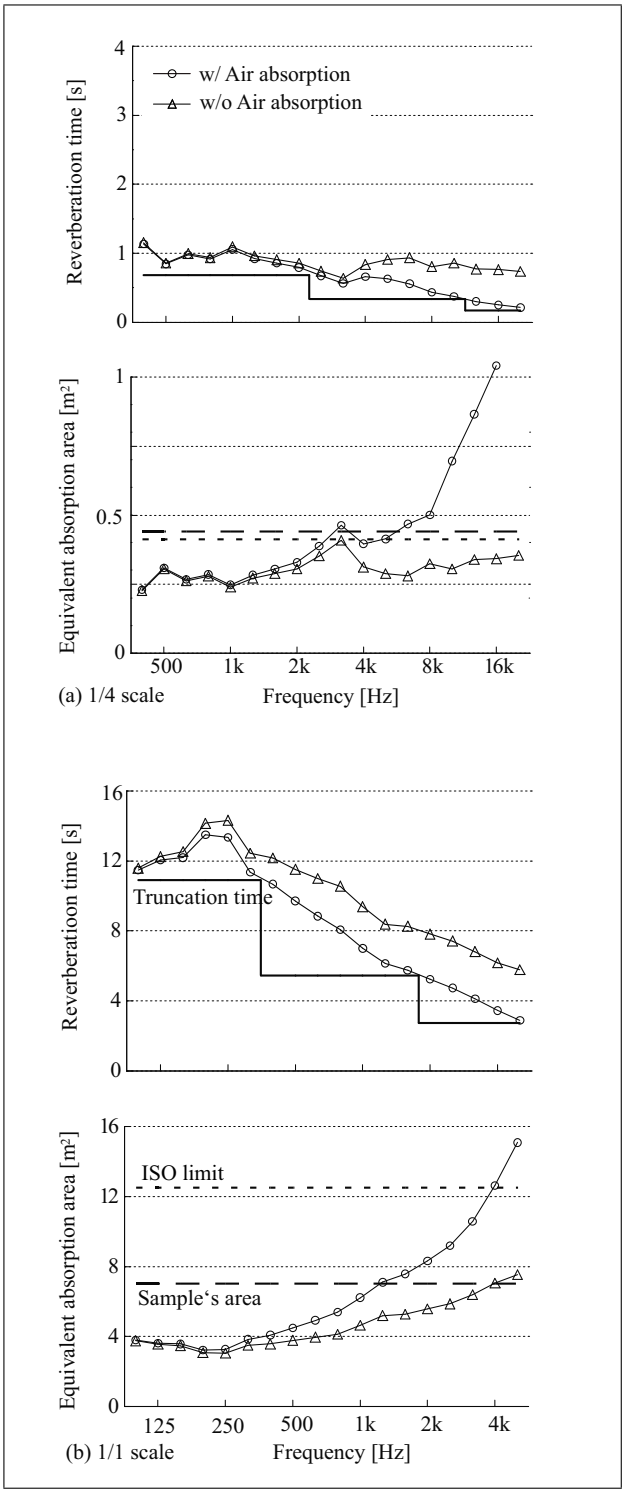


Figure 12. Measured reverberation times and equivalent absorption areas of two reverberation rooms in 1/4 and 1/1 scales.

condition, whereas the 1/4 scale room does not at high frequencies. In comparison with the reverberation times, the signal periods used in 1/4 scale are relatively longer, but not for those in 1/1 scale, especially at low frequencies.

After synchronized averaging of impulse responses, the energy decay curve is obtained by the backward integration method. The ISO standard specifies that the integration limit shall be set at −30 dB, however, in this study

Document downloaded by @DAEL, 2026-11-21 20:54:22 - personal use only

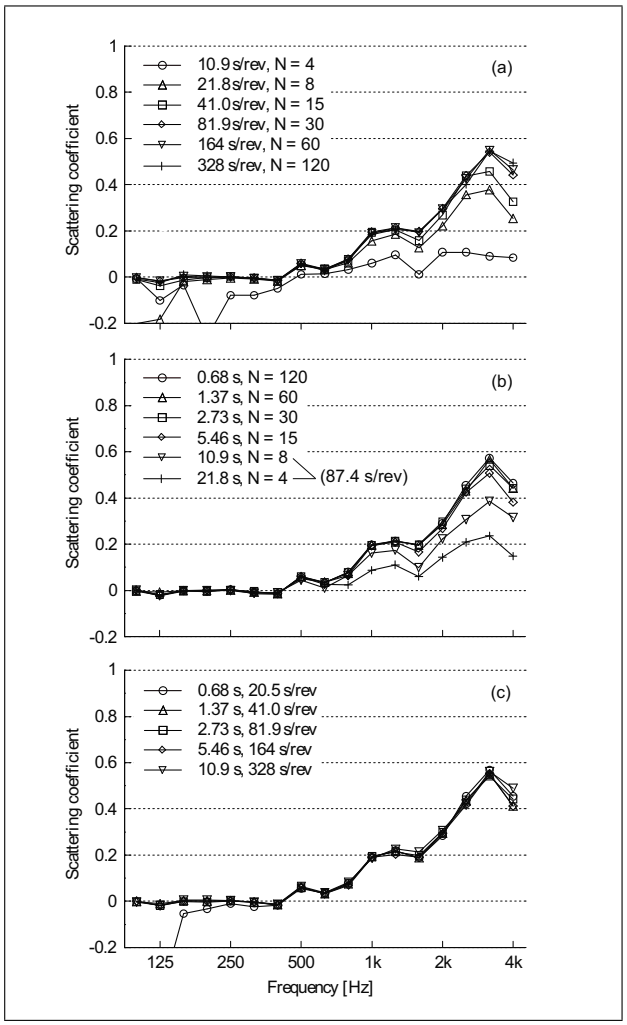


Figure 13. Random-incidence scattering coefficients of the 2D periodic sample, measured with SS signals in 1/4 scale: (a) T_S = 2.73 s, (b) T_R = 81.9 s/rev, and (c) N = 30.

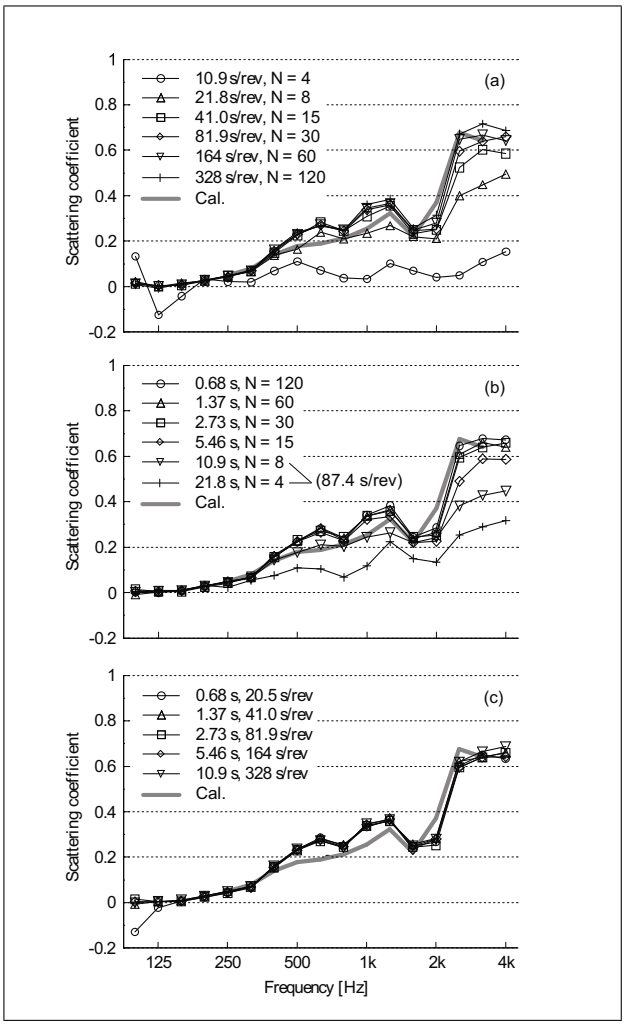


Figure 14. Random-incidence scattering coefficients of the 1D periodic sample, measured with SS signals in 1/4 scale: (a) T_S = 2.73 s, (b) T_R = 81.9 s/rev, and (c) N = 30. Thick lines represent those numerically calculated with the directivity correlation method.

to clarify the effect of different signal periods, a common truncation time is set depending on the reverberation time measured in an empty room. As depicted in Figure 12, the truncation time is fixed at the shortest signal period between $T_1/2$ and T_1 in each 1/3-octave frequency band, which guarantees the integration limit below −30 dB on all conditions. The reverberation times are evaluated by using the least squares estimation of slope in the range from −5 dB to −20 dB, and the arithmetic means of all source-to-receiver paths are calculated.

From the two reverberation times without a test sample, T_1 and T_3, the scattering coefficients for the base plate alone should be checked. It was confirmed that the measured scattering coefficients are below the maximum limits specified by ISO 17497-1 in both scales, excepting at 20 kHz in 1/4 scale, and on the condition with the longest revolution period of 1311 s/rev in 1/1 scale. The former overestimation in 1/4 scale is probably caused by very high air absorption, whereas the latter in 1/1 scale is considered due to time variance of air condition, which suggests that a revolution period of less than about 20 minutes is appropriate in this reverberation room.

4. Measurement results and discussions

4.1. Results in 1/4 scale

Figure 13 shows the random-incidence scattering coefficients of the 2D periodic sample, measured with SS signals on a variety of conditions in 1/4 scale. In the three figures, the following tendencies are observed: (a) at a fixed signal period of 2.73 s, the measured values decrease at higher frequencies, as the revolution period is shorter than 81.9 s/rev (less than 30 signals); (b) at a fixed revolution period of 81.9 s/rev, the values decrease as the signal period is longer than 2.73 s (less than 30 signals); (c) at a fixed number of 30 signals, the values hardly vary regardless of the revolution period and the signal period. On the whole, these tendencies support that the minimum number of signals exists in the use of SS signals, corresponding to the number of angular steps.

In Figure 14, similar tendencies are observed with SS signals for the 1D periodic sample. Additionally, general

Document downloaded by @DAEL, 2026-11-21 20:54:22 - personal use only

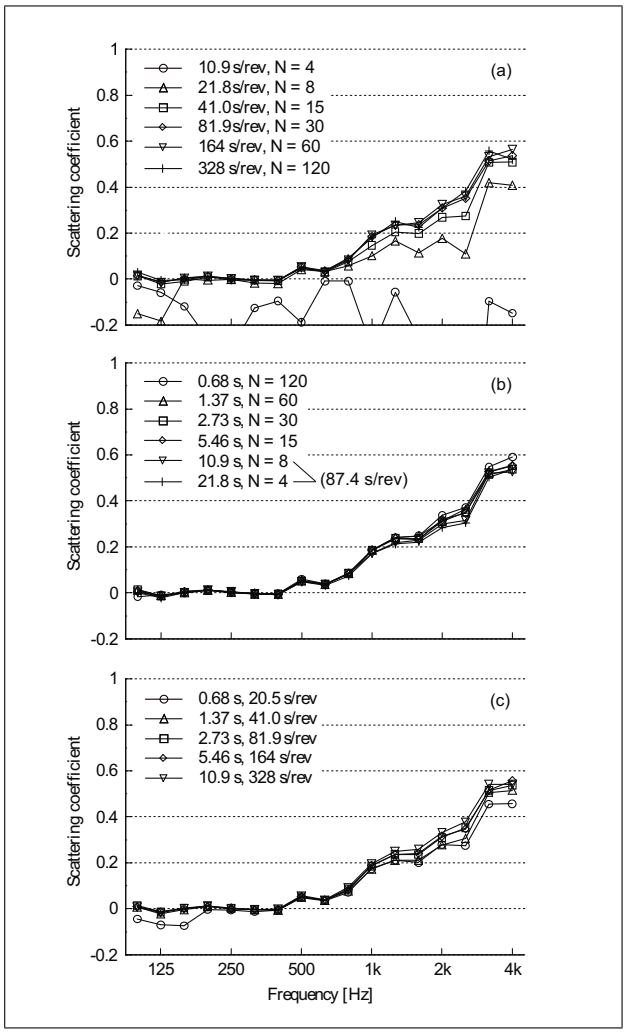


Figure 15. Random-incidence scattering coefficients of the 2D periodic sample, measured with MLS signals in 1/4 scale: (a) $T_S = 2.73$ s, (b) $T_R = 81.9$ s/rev, and (c) $N = 30$.

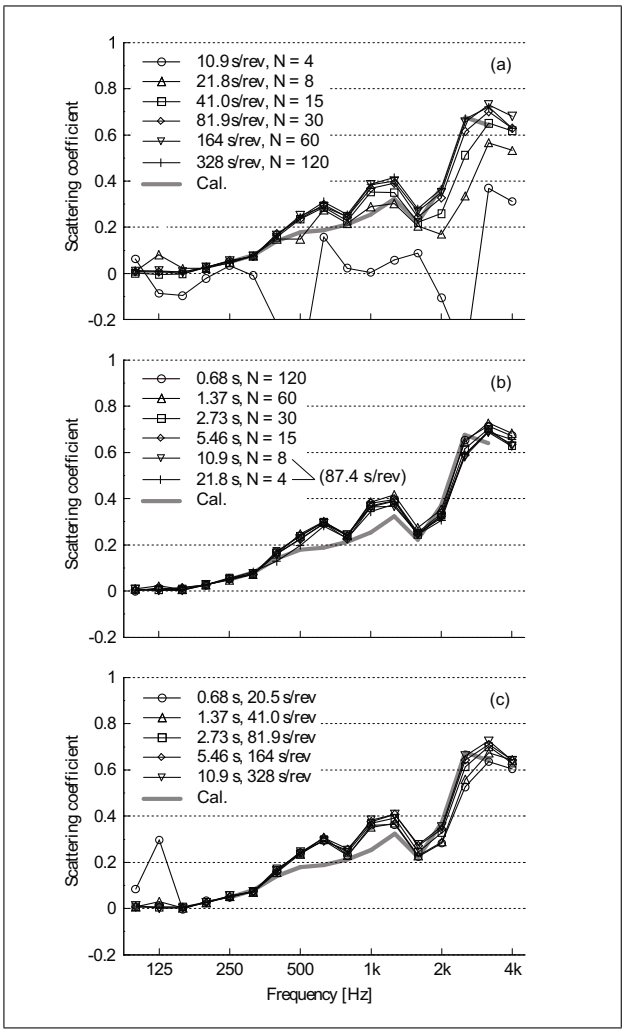


Figure 16. Random-incidence scattering coefficients of the 1D periodic sample, measured with MLS signals in 1/4 scale: (a) $T_S = 2.73$ s, (b) $T_R = 81.9$ s/rev, and (c) $N = 30$. Thick lines represent those numerically calculated with the directivity correlation method.

agreement is seen with numerical results based on the directivity correlation method [19], although involving some discrepancies due to the different method [20]. Closely observing the figure (a), the measured values slightly begin to decrease at 2.5 and 3.15 kHz with the revolution period of 81.9 s/rev (30 signals), which is considered due to higher scattering coefficients. This behavior corresponds to the minimum numbers of steps for ensuring $|\Delta s| \leq 0.05$, that are theoretically estimated on the actual measurement condition (Figure 20a). In this case, the ISO range of $60 \leq N \leq 120$ in the stepwise approach seems to be applicable to the continuous approach using SS signals.

Figures 15 and 16 show the scattering coefficients of the two samples, measured with MLS signals on a variety of conditions. For both samples, the following tendencies are observed: (a) at a fixed signal period of 2.73 s, the measured values decrease at higher frequencies, as the revolution period is shorter than 81.9 s/rev; (b) at a fixed revolution period of 81.9 s/rev, the values hardly vary regardless of the signal period and the number of signals; (c) at a fixed number of 30 signals, the values slightly decrease as the revolution period is shorter than 81.9 s/rev. Regarding the figures (b) and (c), the tendencies are clearly different from those using SS signals. The overall results support that the minimum revolution period exists in the use of MLS signals, and moreover correspond to theoretical estimates for the measurement conditions (Figure 20b).

Figure 17 illustrates examples of energy decay curves after synchronized averaging of impulse responses, measured for the rib structure in the 2.5 kHz frequency band. In the figure (a) where using SS signals with a fixed signal period of 2.73 s (Figure 14a), the overall slope becomes slower with decreasing the revolution period. On the other hand, in the figure (b) where using MLS signals with the same signal period (Figure 16a), the noise floor remarkably goes up, but the initial slope hardly changes with decreasing the revolution period. These different behaviors with SS and MLS signals accord with the theoretical models of the stepwise and the continuous approaches as illustrated in Figures 3 and 6, respectively.

Document downloaded by @DAEL, 2026-11-21 20:54:22 - personal use only

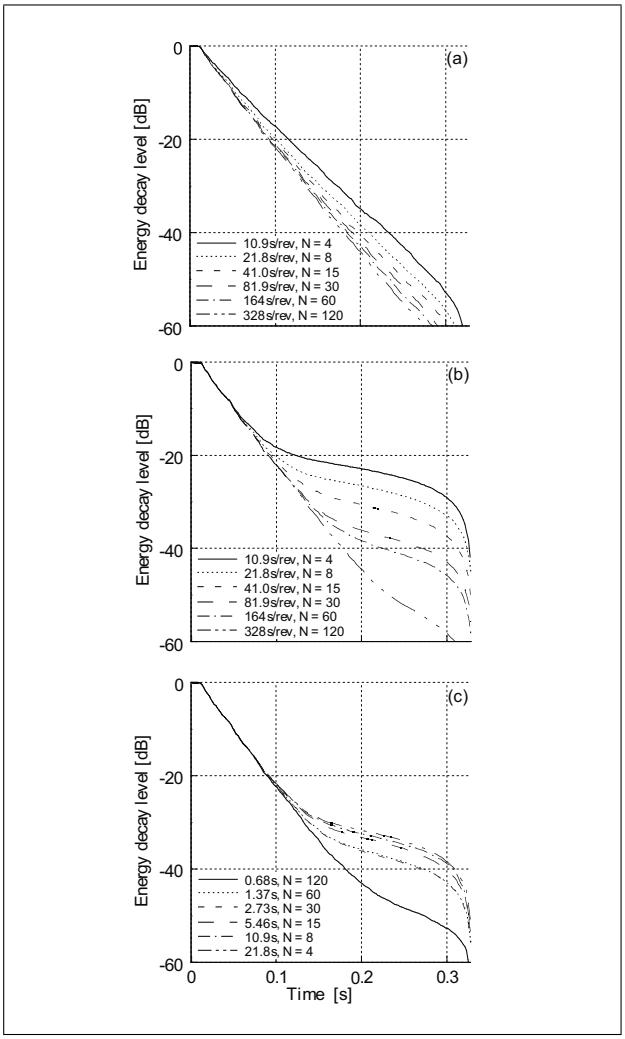


Figure 17. Energy decay curves after synchronized averaging of impulse responses, measured for the 1D periodic sample in the 2.5 kHz frequency band: (a) SS signals with $T_S = 2.73$ s, (b) MLS signals with (b) $T_S = 2.73$ s, and (c) MLS signals with $T_R = 81.9$ s/rev.

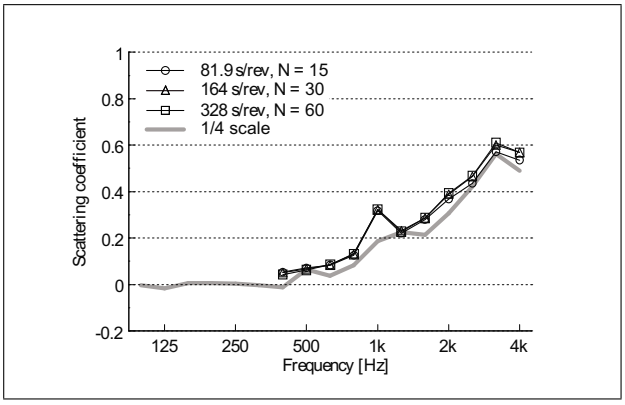


Figure 18. Random-incidence scattering coefficients of the 2D periodic sample, measured with SS signals with $T_S = 5.46$ s in 1/1 scale. A thick line represents typical values measured with SS signals in 1/4 scale.

In the theoretical model of the continuous approach, the energy decay curve depends on the revolution period, but not on the signal period and the number of signals. However, in Figure 17c where using MLS signals with a fixed revolution period of 81.9 s/rev (Figure 16b), the curvature of decay occurs at a little lower level as the signal period is shorter than 5.46 s (more than 15 signals). This tendency can be explained as follows. If the angular interval is smaller than a certain degree, the diffuse component is not completely decorrelated and partially localized in each measurement. As a result, the stationary noise level of the decorrelated part is reduced, while the localized part is diminished in proportion to the specular component by synchronized averaging, similarly to the stepwise approach. Thus it can be stated that, in addition to the minimum revolution period, the use of more signals with a shorter signal period is preferable for MLS signals.

4.2. Results in 1/1 scale

Figure 18 shows the random-incidence scattering coefficients of the 2D periodic sample, measured with SS signals with a fixed signal period of 5.46 s in 1/1 scale. Due to overlapping of successive impulse responses, the measurement is not applicable to the low-frequency bands where the reverberation time of the empty room is longer than twice the signal period. Compared with typical values measured in 1/4 scale, those in 1/1 scale are a little greater, which may be due to the differences in room geometry. Nevertheless, similar to the tendency in 1/4 scale (Figure 13a), the measured values slightly decrease at higher frequencies, as the number of signals is less than 30. Figure 20a also confirms that, in both scales, the theoretical minimum numbers of steps are roughly equal, and 60 signals are sufficient for the sample. As a result, a revolution period of 164 s/rev is applicable for this case.

Figure 19 shows the scattering coefficients of the same sample, measured with MLS signals on a variety of conditions. In the three figures, the following tendencies are observed: (a) at a fixed signal period of 5.46 s, the measured values decrease at higher frequencies, as the revolution period is shorter than 655 s/rev; (b) at a fixed revolution period of 655 s/rev, the values slightly increase as the signal period is shorter; (c) at a fixed number of 60 signals, the values slightly decrease as the revolution period is shorter than 655 s/rev.

Compared with the tendencies in 1/4 scale (Figure 15), those in the figures (a) and (c) are similar, but a little different in the figure (b). Reminding that the minimum revolution period is theoretically proportional to the volume of a room, the different tendency may arise from that the revolution period of 655 s/rev is not sufficient for the 1/1-scale room, due to the relatively large volume. As is seen in Figure 20b, the theoretical minimums for the 1/1-scale room are several times longer than those for the 1/4-scale room with scale conversion. Incidentally, as mentioned in section 3.2, the revolution period of 1311 s/rev is not applicable due to time variance of air condition, thus it will be difficult to find an appropriate revolution speed for a sample of high scattering coefficient in this room.

Document downloaded by @DAEL, 2026-11-21 20:54:22 - personal use only

Table VIII. Tentative minimum absorption areas of the room and the corresponding maximum scattering coefficients of the sample for $N = 60$ and $N = 120$. The maximum absorption areas are quoted from ISO 354.

Frequency [Hz]	100–500	630, 800	1k	1.25k	1.6k	2k	2.5k	3.15k	4k	5k
Max. A_1 [m^2]	6.5	6.5	7.0	7.5	8.0	9.5	10.5	12.0	13.0	14.0
Min. A_1 [m^2]	3.0	4.0	5.0	5.0	6.0	7.0	8.0	9.0	10.0	11.0
Max. s ($N = 60$)	0.40	0.45	0.50	0.50	0.55	0.65	0.65	0.70	0.75	0.80
Max. s ($N = 120$)	0.50	0.60	0.70	0.70	0.80	0.85	0.95	1.00	1.00	1.00

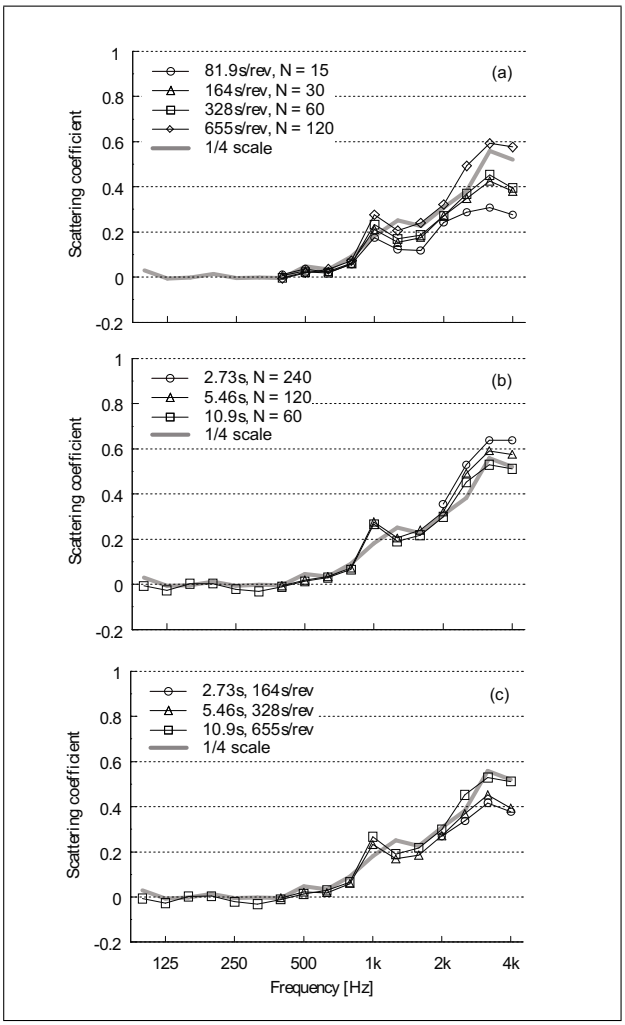


Figure 19. Random-incidence scattering coefficients of the 2D periodic sample, measured with MLS signals in 1/1 scale: (a) $T_S = 5.46$ s, (b) $T_R = 655$ s/rev, and (c) $N = 60$. Thick lines represent typical values measured with MLS signals in 1/4 scale.

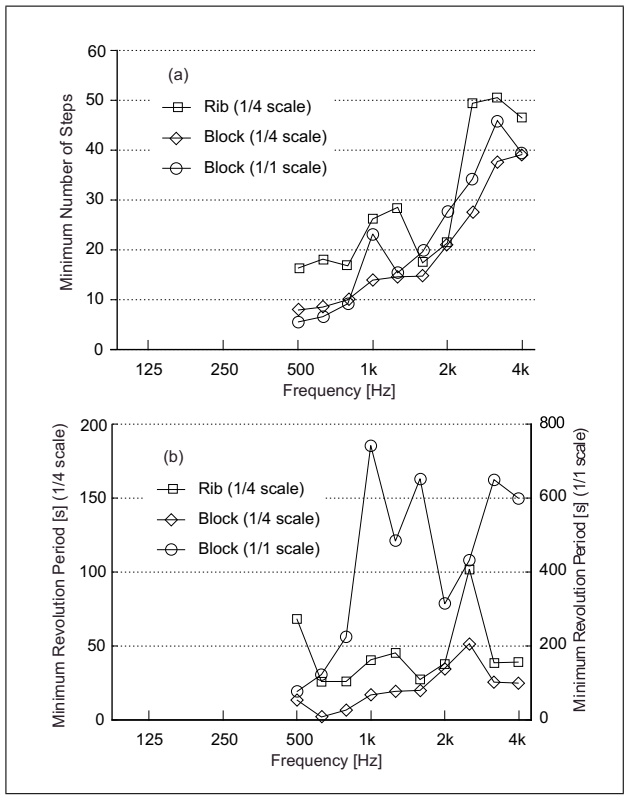


Figure 20. Theoretical estimates of requirements, that ensures $|\Delta s| \leq 0.05$ for the measurement conditions in 1/4 and 1/1 scales: (a) the minimum number of steps N, and (b) the minimum revolution period T_R.

5. Conclusions

In the reverberation room method for measuring scattering coefficients, a sample rotation scheme is employed where synchronized averaging of room impulse responses is performed during stepwise or continuous rotation of a test sample. In practice, the two alternative approaches are performed using periodic pseudo-random or time modulated signals, typically maximum-length sequence or swept sine. Naturally, the choice of signals does not affect the results in the stepwise approach. On the other hand, it was theoretically shown that the continuous approach with MLS signals causes different systematic error to the stepwise approach, but the continuous approach with SS signals is almost equivalent to the stepwise approach. Furthermore, the requirements of the continous approach with MLS signals differ from the other approaches in the dependence of the sample's scattering coefficient and the room's absorption area. Significant features of the above approaches are as follows:

- The stepwise approach has the minimum number of angular steps, regardless of signals types, which increases as the sample's scattering coefficient is higher and the room's absorption area is smaller.
- The continuous approach with SS signals has the minimum number of signals per revolution, which is equal to that of angular steps in the stepwise approach.
- The continuous approach with MLS signals has the minimum revolution period, proportional to the room

Document downloaded by @DAEL, 2026-11-21 20:54:22 - personal use only

volume, and rather affected by the truncation time of impulse responses. It also increases as the sample's scattering coefficient is higher and the room's absorption area is smaller.

The minimum number of steps and the minimum revolution period were theoretically formulated, and roughly validated through small- and full-scale experiments.

Regarding test signals, it can be concluded that the use of SS signals is generally preferable to MLS signals in the continuous approach. With SS signals, accuracy control by the number of signals is easier and more reliable, regardless of room volume. In addition, a common minimum number can be provided for the two alternative approaches. In the current ISO 17497-1, the use of MLS signals is recommended, and more problematically, without any limitation of revolution speed. With MLS signals, accuracy can be controlled by the revolution period, however it is troublesome due to the dependence on room volume and impulse response truncation.

In theory, systematic underestimation is reduced with more absorptive room, however in reality, other uncertainties in the reverberation time determination certainly cause greater error. Consequently, there will be an appropriate range of equivalent absorption area for the reverberation room. Considering that the equivalent absorption area increases at higher frequencies due to air absorption, it is quite favorable for actual measurement, since the scattering coefficient generally tends to increase at higher frequencies. Nevertheless, in the stepwise or the continuous approach with swept sine signals, the current ISO range from 60 to 120 angular steps can yield a significant underestimation for a high scattering coefficient in a reverberation room satisfying the maximum absorption areas in ISO 354. As an attempt, Table VIII shows the maximum scattering coefficients for the lower and the upper limits of steps, theoretically estimated to ensure an underestimation of less than 0.5, with tentative minimum absorption areas for the room. For better measurement accuracy, one possible way is to add a minimum equivalent absorption area of the empty room and the corresponding upper limit of scattering coefficient in each frequency band.

Acknowledgement

The authors are very grateful to Mr. Yuzo Tsuchiya (Toda Corp.) and Mr. Yoshikazu Honji (Yamaha Corp.) for their assistance with the measurements. This project has been funded by the Grant-in-Aid Scientific Research from Japan Society for the Promotion of Science (No. 21360275).

References

[1] T. J. Cox, P. D'Antonio: Acoustic absorbers and diffusers. 2nd ed., chap. 2. Taylor and Francis, London, 2009.

[2] T. J. Cox, B.-I. L. Dalenbäck, P. D'Antonio, J.-J. Embrechts, J. Y. Jeon, E. Mommertz, M. Vorländer: A tutorial on scattering and diffusion coefficients for room acoustic surfaces. Acta Acustica united with Acustica **92** (2006) 1–15.

[3] M. Vorländer, E. Mommertz: Definition and measurement of random-incidence scattering coefficients. Appl. Acoust. **60** (2000) 187–199.

[4] E. Mommertz: Determination of scattering coefficients from the reflection directivity of architectural surfaces. Appl. Acoust. **60** (2000) 201–203.

[5] M. Vorländer: International round robin on room acoustical computer simulations. Proc. 15th ICA, 1995, Vol. II, 689–692.

[6] I. Bork: A comparison of room simulation software. The 2nd round robin on room acoustical computer software. Acustica united with Acta Acustica **86** (2000) 943–956.

[7] C. L. Christensen: Odeon room acoustics program ver. 11. User manual: Industrial, auditorium and combined editions. Odeon A/S, Lyngby, Denmark, 2011.

[8] B.-I. Dalenbäck: CATT-acoustic ver. 9. User's manual. CATT, Gothenburg, 2011.

[9] ISO 17497-1: Acoustics – Sound-scattering properties of surfaces – Part 1: Measurement of the random-incidence scattering coefficient in a reverberation room. 2004.

[10] J. Embrechts: Practical aspects of the ISO procedure for measuring the scattering coefficient in a real-scale experiment. Proc. Forum Acusticum, Sevilla, 2002, RBA–06–001–IP.

[11] M. H. Gomes, M. Vorländer, S. Gerges: Aspects of the sample geometry in the measurement of the random-incidence scattering coefficient. Proc. Forum Acusticum, Sevilla, 2002, RBA–06–002–IP.

[12] L. De Geetere, G. Vermeir: Investigations on real-scale experiments for the measurement of the ISO scattering coefficient in the reverberation room. Proc. Forum Acusticum, Sevilla, 2002, RBA–06–004–IP.

[13] M. Vorländer, J.-J. Embrechts, L. De Geetere, G. Vermeir, M. H. Gomes: Case studies in measurements of random incidence scattering coefficient. Acta Acustica united with Acustica **90** (2004) 858–867.

[14] Y.-J. Choi, D.-U. Jeong: Some issues in measurement of the random-incidence scattering coefficients in a reverberation room. Acta Acustica united with Acustica **94** (2008) 769–773.

[15] Y.-J. Choi, D.-U. Jeong: Effects of unspecified experimental conditions in ISO 17497-1 on the scattering coefficients measured in a scale model. Acta Acustica united with Acustica **97** (2011) 75–81.

[16] ISO 354: Acoustics – Measurement of sound absorption in a reverberation room. 2003.

[17] M. Vorländer, M. Kob: Practical aspects of MLS measurements in building acousitcs. Appl. Acoust. **52** (1997) 239–258.

[18] U. P. Svensson, J. L. Nielsen: Errors in MLS measurements caused by time variance in acoustic systems. J. Audio Eng. Soc. **47** (1999) 907–927.

[19] Y. Kosaka, T. Sakuma: Numerical examination on the scattering coefficients of architectural surfaces using the boundary element method. Acoust. Sci. Tech. **26** (2005) 136–144.

[20] T. Sakuma, Y. Kosaka, L. de Geetere, M. Vorländer: Relationship between the scattering coefficients determined with coherent averaging and with directivity correlation. Acta Acustica united with Acustica **95** (2009) 669–677.

[21] J. Y. Jeon, S. C. Lee, M. Vorländer: Development of scattering surfaces for concert halls. Appl. Acoust. **65** (2004) 341–355.

[22] Y. H. Kim, H. S. Jang, J. Y. Jeon: Characterizing diffusive surfaces using scattering and diffusion coefficients. Appl. Acoust. **72** (2011) 899–905.

[23] F.-M. Lin, P.-Y. Hong, C.-Y. Lee: An experimental investigation into the sound-scattering performance of wooden diffusers with different structures. Applied Acoustics **71** (2010) 68–78.

Document downloaded by @DAEL, 2026-11-21 20:54:22 - personal use only